Migration of human melanoma cells depends on extracellular pH and Na^+/H^+ exchange

Christian Stock[1], Birgit Gassner[2], Christof R. Hauck[3], Hannelore Arnold[1], Sabine Mally[1], Johannes A. Eble[4], Peter Dieterich[5] and Albrecht Schwab[1]

[1] *Institute of Physiology II, University of Münster, Robert-Koch-Str.27b, D-48149 Münster, Germany*
[2] *Physiologisches Institut, University of Würzburg, Röntgenring 9, D-97070 Würzburg, Germany*
[3] *Zentrum für Infektionsforschung, University of Würzburg, Röntgenring 11, D-97070 Würzburg, Germany*
[4] *Institute for Physiological Chemistry und Pathobiochemistry, Münster University Hospital, Waldeyerstr. 15, D-48149 Münster, Germany*
[5] *Physiologisches Institut, Medizinische Fakultät Carl-Gustav-Carus, Fetscher-Str. 74, D-01307 Dresden, Germany*

Their glycolytic metabolism imposes an increased acid load upon tumour cells. The surplus protons are extruded by the Na^+/H^+ exchanger (NHE) which causes an extracellular acidification. It is not yet known by what mechanism extracellular pH (pH_e) and NHE activity affect tumour cell migration and thus metastasis. We studied the impact of pH_e and NHE activity on the motility of human melanoma (MV3) cells. Cells were seeded on/in collagen I matrices. Migration was monitored employing time lapse video microscopy and then quantified as the movement of the cell centre. Intracellular pH (pH_i) was measured fluorometrically. Cell–matrix interactions were tested in cell adhesion assays and by the displacement of microbeads inside a collagen matrix. Migration depended on the integrin $\alpha2\beta1$. Cells reached their maximum motility at pH_e ~7.0. They hardly migrated at pH_e 6.6 or 7.5, when NHE was inhibited, or when NHE activity was stimulated by loading cells with propionic acid. These procedures also caused characteristic changes in cell morphology and pH_i. The changes in pH_i, however, did not account for the changes in morphology and migratory behaviour. Migration and morphology more likely correlate with the strength of cell–matrix interactions. Adhesion was the strongest at pH_e 6.6. It weakened at basic pH_e, upon NHE inhibition, or upon blockage of the integrin $\alpha2\beta1$. We propose that pH_e and NHE activity affect migration of human melanoma cells by modulating cell–matrix interactions. Migration is hindered when the interaction is too strong (acidic pH_e) or too weak (alkaline pH_e or NHE inhibition).

(Received 9 April 2005; accepted after revision 8 June 2005; first published online 9 June 2005)
Corresponding author C. Stock: Institute of Physiology II, University of Münster, Robert-Koch-Str.27b, D-48149 Münster, Germany. Email: cmstock@uni-muenster.de

Cell migration away from the primary tumour is a major step in metastasis. This multistep process requires sequential interaction between the invasive cell and the surrounding extracellular matrix. It is based on (i) extracellular matrix proteolysis by matrix metalloproteinases (Egeblad & Werb, 2002), (ii) directed reorganization of the cytoskeleton (Mitchison & Cramer, 1996), (iii) activity of ion channels and transporters such as Na^+/H^+ or Cl^-/HCO_3^- exchangers (Klein *et al.* 2000; Schwab, 2001; Denker & Barber, 2002*a*,*b*; Saadoun *et al.* 2005), and (iv) a coordinated formation and release of focal adhesion contacts to the extracellular matrix mediated by integrin receptor molecules (Beningo *et al.* 2001; Jalali *et al.* 2001; Webb *et al.* 2002).

Focal adhesion contacts are stable cell–substrate interactions evolving from focal complexes which are characterized as small and transient cell interactions between the cell and the extracellular matrix (Friedl & Wolf, 2003). Focal contacts comprise integrins, the focal adhesion kinase (FAK), talin, vinculin, paxillin and other proteins attached to the actin filament network (Brakebusch & Fässler, 2003). The ubiquitously expressed Na^+/H^+ exchanger isoform, NHE1, is also part of these focal contacts at which it may directly interact with integrins (Schwartz *et al.* 1991; Grinstein *et al.* 1993; Plopper *et al.* 1995). In fibroblasts, NHE1 anchors the actin cytoskeleton to the plasma membrane by its direct binding of ERM proteins (Denker *et al.* 2000; Denker & Barber, 2002*a*). A loss of this NHE1-dependent cytsokeletal anchoring impairs cell polarity and reduces the directionality in cell migration (Denker & Barber, 2002*b*). The transport activity of the NHE1 is stimulated

 DOI: 10.1113/jphysiol.2005.088344

during cell adhesion (Schwartz, 1992; Schwartz & Lechene, 1992) and is necessary for the assembly of focal adhesions (Tominaga & Barber, 1998).

However, the primary task of the NHE1 is the regulation of intracellular pH (pH_i) and cell volume. NHE1 activity is of importance for many tumour cells (Lagarde *et al.* 1988; Rotin *et al.* 1989; Tannock & Rotin, 1989; McLean *et al.* 2000). The insufficient and/or inefficient tumour vascularization leads to a diminished O_2 supply so that the metabolism of tumour cells is mostly glycolytic (Gulledge & Dewhirst, 1996; Helmlinger *et al.* 2002). Thus, tumour cells are often challenged by an increased acid load (Griffiths, 1991). The excess protons are extruded into the extracellular space by transport proteins such as the NHE1 (Yamagata & Tannock, 1996; Wahl *et al.* 2002) which then causes an acidification of the extracellular space (Tannock & Rotin, 1989). The role of the extracellular pH (pH_e) in tumour cell migration, however, has not yet been established. NHE activation enhances the invasiveness of human breast cell carcinoma cells (Reshkin *et al.* 2000) implying a possible involvement of NHE and extracellular pH (pH_e) in metastasis and tumour malignancy. We therefore investigated whether pH_e and NHE activity modulate the motility of human melanoma cells *on* collagen matrices as well as *in* three-dimensional collagen lattices.

Methods

Cells and cell culture

The melanoma cell line MV3 (Van Muijen *et al.* 1991) was grown in bicarbonate-buffered RPMI 1640 (Sigma, Taufkirchen, Germany) supplemented with 10% (v/v) fetal bovine serum (FBS) at 37°C in a humidified atmosphere of 5% CO_2. Confluent MV3 cells were either plated onto (two-dimensional migration, 2D; for further details see below) or incorporated into (three-dimensional migration, 3D) collagen matrices except where stated otherwise.

Experimental solutions

Depending on the experimental set-up (experimental chamber airtight (5% CO_2, 2D experiments) or open (0.03% CO_2, 3D experiments)), experimental solutions and media were buffered with either $NaHCO_3$ (2D) or with Hepes (3D). The amount of $NaHCO_3$ to be added to the media was determined by the desired pH value.

Measurements of the intracellular pH were performed using Hepes-buffered Ringer solutions of different pH values containing (mmol l^{-1}): 122.5 NaCl, 5.4 KCl, 0.8 $MgCl_2$, 1.2 $CaCl_2$, 1.0 $NaH_2PO_4.2H_2O$, 5.0 glucose, 10 Hepes. The pH was adjusted by adding 1 M NaOH. Phosphate-buffered saline (PBS) solution was used as solvent for the antibodies and as washing buffer as well. The PBS contained (mmol l^{-1}): 137 NaCl, 2.7 KCl, 8.1 Na_2HPO_4, 1.5 KH_2PO_4.

When applicable the NHE inhibitors ethylisopropylamiloride (EIPA; final concentration: 10 μmol l^{-1} in 0.05% ethanol) or HOE642 (Cariporide; final concentration: 10 μmol l^{-1}) were added. Rhodocetin, a component of snake venom that binds highly specifically to the integrin dimer $\alpha2\beta1$ over a broad pH range (Eble & Tuckwell, 2003) was applied in a concentration of 5 μg ml^{-1}.

Antibodies

The monoclonal anti-hVin-1 (Sigma, Saint Louis, MO, USA) and the function blocking anti-human integrin $\beta1$ (4B7R) (Santa Cruz Biotechnology, Inc., Sant Cruz, CA, USA; Friedlander *et al.* 1996) were used for immunolabelling. Immunoblotting was performed with the anti-human integrin $\beta1$ from Chemicon International (Temecula, CA, USA). A Cy3-conjugated goat anti-mouse IgG or a horseradish peroxidase-conjugated goat anti-mouse IgG (both from Jackson ImmunoResearch Laboratories, West Grove, PA, USA) served as the secondary antibodies.

Preparation of collagen matrices

One hundred mirolitres of 10× $RPMI^-$ 1640 and 100 μl 10× Hepes buffer (final Hepes concentration: 10 mmol l^{-1}) were added to 800 μl collagen G solution (Biochrom AG, Berlin, Germany). When cells were embedded in collagen lattices for three-dimensional (3D) experiments the different pH_e values were adjusted prior to the polymerization process by adding various amounts of 1 M NaOH. The cell density was kept at 250 000 cells ml^{-1}. This cell-containing collagen solution polymerized within 3 h at 37°C in an open experimental chamber. When cell migration was observed on collagen matrices (2D) the pH of the cell free collagen mixture was always adjusted to pH 7.4 bearing in mind that the polymerization and self-assembly of collagen may be affected by the concentration of free protons (Williams *et al.* 1978; Freire & Coelho-Sampaio, 2000). An ensured reproducible collagen polymerization leading to a consistently fibrous matrix structure enabled us to exclude that the observed effects are based on pH-dependent differences in the matrix. The bottoms of culture flasks (12.5 cm^2, Falcon) were covered with 500 μl collagen solution. About 100 μl of the same collagen solution were filled in a 1.5 ml Eppendorf tube in order to confirm the final pH of the gel after its polymerization by using a small pH electrode (Mettler, Toledo, Switzerland). The collagen was allowed to polymerize overnight at 37°C. Cells were seeded on this collagen matrix

and allowed to adapt to different pH values varying from 6.4 to 7.5 for 3 h prior to recording.

The tractive power exerted by cells pulling on collagen fibrils was visualized by incorporating fluorescent microspheres (FluoSpheres, 1 μm, Molecular Probes, Inc., Eugene, OR, USA) into the collagen matrix at a concentration of 4×10^7 beads ml^{-1} (Tamariz & Grinnell, 2002).

Videomicroscopy and computer-assisted cell tracking

The culture flasks (2D) or experimental chambers (3D) were put in heated chambers on stages of inverted microscopes (ID03 and Axiovert25, Carl Zeiss, Inc., Göttingen, Germany). Cell migration was recorded for 5 h at 37°C using video cameras (Models XC-ST70CE and XC-77CE, Hamamatsu/Sony, Japan) and PC-vision frame grabber boards (Hamamatsu). Images were taken in 10 min intervals controlled by a high performance image control system (HiPic, Hamamatsu Photonics Deutschland GmbH, Herrsching, Germany). The circumferences of the cells were labelled employing the AMIRA software (TGS Inc., San Diego, CA, USA). The cell contours then served as the basis for further analysis. Each cell that remained in the visual field during the experiment without dividing or colliding with another cell was evaluated. Parameters such as the cell area, the structural index (SI) and the migratory speed were analysed using self-made JAVA programs and the NIH ImageJ software (http://rsb.info.nih.gov/ij/). Migration was determined as the movement of the cell centre per time unit, the speed was estimated from the 10 min time interval applying a three point difference quotient and the cell area was measured as the number of pixels. The structural index (SI) represents the cell shape. SI was calculated as follows:

$$\mathrm{SI} = (4\pi A)/p^2$$

where A is the area covered by the cell and p is the perimeter of A (Dunn & Brown, 1987, 1990). Values close to '1' correspond to a spherical cell shape whereas values close to '0' correspond to a spindle or a dendritic cell shape.

Measuring the intracellular pH (pH_i)

pH_i of MV3 cells was measured using video imaging techniques and the fluorescent pH indicator BCECF (Molecular Probes, OR, USA). Cells were treated as for migration experiments. They were resuspended in one of the Hepes-buffered experimental solutions containing EIPA or HOE642 where applicable. They were plated onto collagen coated coverslips and allowed to adapt for 3 h. Cells were then incubated in the respective experimental solution containing 2 μmol l^{-1} BCECF-AM for 1–2 min. The coverslips were placed on the stage of an inverted microscope (Axiovert TV 100; Carl Zeiss, Inc., Göttingen, Germany) and continuously superfused with prewarmed Hepes-buffered Ringer solution. The excitation wavelength alternated between 488 and 460 nm, respectively, while the emitted fluorescence was monitored at 500 nm using an ICCD camera (Atto Bioscience, Rockville, MD, USA). Filter change and data acquisition were controlled by Attofluor software (Atto Bioscience). Fluorescence intensities were measured in 10 s intervals and corrected for background fluorescence. At the end of each experiment, the pH_i measurements were calibrated by successively superfusing the MV3 cells with modified Ringer solutions of pH 7.5, 7.0 and 6.5 containing (mmol l^{-1}): 125 KCl, 1 $MgCl_2$, 1 $CaCl_2$, 20 Hepes, and 10 μmol l^{-1} nigericin (Sigma).

Cell adhesion

MV3 cells were resuspended in serum free RPMI media (RPMI$^-$) of different pH (pH 6.4 to pH 7.5) with or without 10 μmol l^{-1} EIPA. Cells were then seeded in collagen (4 mg ml^{-1}) coated 24-well plates at a density of 30 000 cells per well. After 60 min the media including the non-adhesive cells were removed. The remaining cells were washed with cold PBS buffer, then fixed and counted. In addition to their number the cells' morphology given as structural index (SI) and cell area was evaluated as described above. The software MetaVue (Universal Imaging) was used for taking images and counting.

Western blot of integrin β1

Confluent cells were transferred into serum-free bicarbonate-buffered RPMI 1640 medium of various pH values (7.5, 7.0 and 6.6) and allowed to adapt for ~15 h. They were then washed with cold PBS and lysed at 4°C in lysis buffer containing (mmol l^{-1}): 150 NaCl, 5.0 EDTA, 50 Tris-HCl (pH 7.5) and 1.0 Pefabloc SC Plus (Roche Molecular Biochemicals, Mannheim, Germany), 1% Triton X-100, and 0.2% (v/v) of a protease inhibitor cocktail (Sigma, P 8340). Lysates were scraped off 10 cm culture dishes (Falcon) and mixed with reducing sample buffer (4 : 1, v/v) containing 500 mmol l^{-1} Tris, 100 mmol l^{-1} dithiothreitol, 8.5% SDS, 27.5% sucrose and 0.03% bromophenol blue indicator. SDS-PAGE was performed using acrylamide gels (7.5%) and a Minigel System (Bio-Rad Laboratories, Hercules, CA, USA). Equal amounts of protein (~2 μg) were loaded. Electroblotting was performed at 0.8 mA cm^{-2} gel for 50 min. The nitrocellulose membranes (Schleicher & Schuell, Dassel, Germany) carrying the blotted proteins were bathed in 5% (w/v) milk in 0.1% (v/v) Tween in PBS for 1 h at room temperature and then washed with 0.1% Tween in PBS. Overnight incubation with the primary antibody

(1 : 600) at 4°C was followed by a 1 h incubation with a horseradish peroxidase-conjugated secondary antibody (1 : 50 000) at room temperature. Blots were developed using an ECL immunoblotting detection reagent kit (Amersham, Arlington Heights, IL, USA). In order to quantify β1 integrin expression, five blots were scanned and the number of pixels representing a marked band area was multiplied by the band's mean grey value calculated by the NIH ImageJ software.

Immunofluorescence

Cells were treated with cold 1% Triton X-100 in PBS for 10 min prior to fixation. Without this prepermeabilization step vinculin could hardly be labelled as the epitope was not accessible enough to the antibody. Cells were then fixed by 3.5% paraformaldehyde in PBS. Non-specific binding sites were blocked using 100 mM glycine in PBS and 10% (v/v) goat normal serum in PBS. After staining the cells with the hVIN-1 mAb or the integrin β1 (4B7R) mAb for 1 h and a Cy3-conjugated IgG for another hour (in a dilution of 1 : 800 each), the slide preparations were fixed once again, washed in PBS and then covered with Vectashield (Vector Laboratories Inc., Burlingame, CA, USA). Images were taken using an invert microscope (Axiovert200, Carl Zeiss, Inc., Göttingen, Germany), a digital camera (Model 9.0, RT-SE-Spot, Visitron Systems) and the MetaVue software.

Statistics

All experiments were repeated three to six times. Data are presented as the mean values ± S.E.M. The data were tested for significance employing Student's unpaired *t* test or analysis of variance (ANOVA) where applicable. The level of significance was set at $P < 0.01$ except where otherwise stated.

Results

Cell migration depends on pH_e and NHE activity

We calculated the average speed (given in μm min^{-1}; Fig. 1*A* and *C*) and the mean translocation (= distance covered within 5 h; Fig. 1*B*, *D* and *E*) of migrating MV3 cells. Cells seeded on collagen (Fig. 1*A*) reached their maximum speed of 0.68 ± 0.03 μm min^{-1} at pH_e 7.0 ($n = 30$ cells from three to five trials in each case). An increase in pH_e to pH 7.5 or a decrease to pH 6.4 caused the migratory speed to decrease almost linearly to 0.11 ± 0.01 μm min^{-1} and 0.24 ± 0.02 μm min^{-1}, respectively. The cells covered 109.9 ± 15.1 μm at pH_e 7.0, but only 20.7 ± 2.8 μm and 27.2 ± 5 μm at pH_e 7.5 and pH_e 6.6, respectively (Fig. 1*B* and *E*). NHE inhibition by EIPA or HOE642 decreased speed and translocation by up to 70% at pH_e 7.0 (0.2 ± 0.02 μm min^{-1}, 28 ± 3.7 μm within 5 h). Extracellular acidification to pH_e 6.8 did not amplify the inhibitory effect of NHE blockage on cell migration. However, migration was inhibited when cells were exposed to propionic acid (15 mmol l^{-1}) while the extracellular pH was kept constant at pH_e 7.0. Protonated weak organic acids such as propionic acid permeate the plasma membrane and dissociate rapidly in the cytosol causing an initial intracellular acidification and an increase in NHE activity (Boron, 1983; Klein *et al.* 2000). After a 3 h exposure of MV3 cells to 15 mmol l^{-1} sodium propionate at a constant pH_e of 7.0 and a pH_i of 7.1 ± 0.05 ($n = 38$ cells from four trials, for details see below) the migratory speed on a 2D matrix was reduced to 0.07 ± 0.01 μm min^{-1} ($n = 36$ cells from eight different trials). The translocation within 5 h was only 18.5 ± 2.77 μm (cf. Fig. 1*A* and *B*). Additional exposure of acidified cells to 10 μmol l^{-1} HOE642 led to a further decrease in the migratory speed (0.03 ± 0.004 μm min^{-1}, $n = 40$ cells from 4 different trials, cf. Fig. 1*A* and *B*) and the cells' translocation (6.45 ± 0.9 μm (5 h)$^{-1}$).

Cells embedded in three-dimensional collagen lattices (Fig. 1*C* and *D*) behaved similarly ($n = 10$–20 cells from three to five trials in each case). They reached their maximum speed and translocation at pH_e 7.18: 0.46 ± 0.03 μm min^{-1} and 112.9 ± 15.5 μm ($n = 16$; Supplemental material video 1). When pH_e was reduced to pH 6.75 (video 2) or increased to pH 8.1 (video 3) migratory speed and translocation decreased significantly (at pH_e 6.75: 0.12 ± 0.01 μm min^{-1} and 8.2 ± 1.8 μm ($n = 10$); at pH_e 8.1: 0.14 ± 0.02 μm min^{-1} and 13.6 ± 2.7 μm ($n = 15$)). NHE inhibition by EIPA (video 4) or HOE642 (Cariporide; video 5) decreased speed and translocation by 55%: 0.20 ± 0.02 μm min^{-1} and 20.6 ± 4.6 μm (EIPA; $n = 20$), and 0.18 ± 0.02 μm min^{-1} and 26.7 ± 4.3 μm (HOE642, $n = 20$). HOE642 inhibits cell migration (Fig. 2*A* and *B*) at pH_e 7.0 with an IC_{50} of $\sim$5 μmol l^{-1} and affects cell morphology (Fig. 2*C*) in a dose-dependent manner indicating that NHE activity plays a major role in controlling cell migration and morphology. Most likely it is the isoform NHE1 as revealed by Western blot analysis (data not shown). Also, at the concentration used in this study HOE642 is unlikely to effectively inhibit the resistant NHE isoforms such as NHE3 (Scholz *et al.* 1995). The IC_{50} value for HOE642 effects on the human NHE3 is 900 μmol l^{-1} (Schwark *et al.* 1998).

Speed and translocation were reduced to a similar extent when the integrin dimer $\alpha 2\beta 1$ was specifically blocked by rhodocetin (Fig. 1). Moreover, Table 1 shows that, regardless of pH_e, cells seeded on poly L-lysine hardly migrated and that they did not spread but remained spherical. These observations confirm the finding by Maaser *et al.* (1999) that in MV3 cells the integrin $\alpha 2\beta 1$ is indispensable for cell migration on collagen.

Cell morphology is determined by pH_e and/or by NHE activity

Since changes in motility and migratory behaviour might be accompanied by morphological modifications we checked whether pH_e and NHE activity also affected the cell morphology. As shown in Fig. 3, cells were dendritic at pH_e 6.6 or of ameboid shape at pH_e 7.0 whereas they were spherical at pH_e 7.5 (2D) or pH_e 8.1 (3D) and in the presence of NHE inhibitors. These morphological properties were quantified by calculating the structural index (SI) and counting the lamellipodia per cell ($n =$ 30 cells from five trials in each case) 60 min after seeding

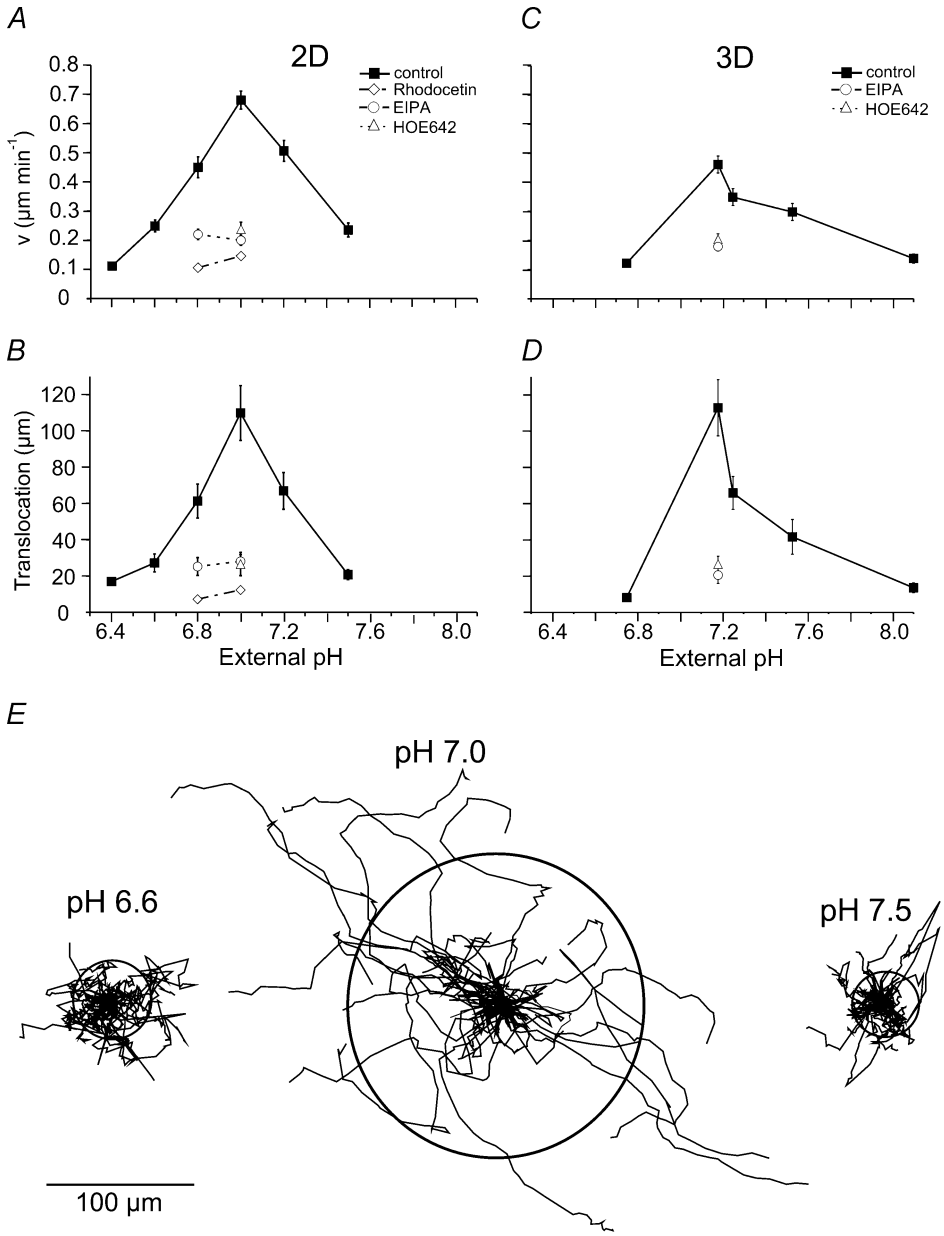

Figure 1. Migratory speed, translocation and trajectories of MV3 cells depend on pH_e
Cells were either seeded *on* collagen matrices (2D: *A*, *B* and *E*) or incorporated *in* collagen lattices (3D: *C* and *D*; Supplemental material video 1; video 2; video 3) and recorded for 5 h. Migratory speed (*A* and *C*) and translocation within 5 h (*B* and *D*) under control conditions (■), after the application of EIPA (○; video 4) or HOE642 (△ ; video 5) and upon treatment with rhodocetin (grey diamonds). *n* varied between 30 (2D) and 10–20 (3D) cells taken from three to five different trials. *E*, trajectories of MV3 cells migrating *on* collagen (2D) at different pH_e values. Trajectories obtained under the same experimental conditions were standardized. They all begin at the same starting post represented by the centre of a circle. The radii of the circles represent the mean distances covered within 5 h. $n = 30$ cells each, taken from three to five different trials.

*on*to collagen (Fig. 4). SI dropped from 0.82 ± 0.02 to 0.33 ± 0.03 as pH_e decreased from pH 7.5 to pH 6.6. It then rose to 0.73 ± 0.03 as pH_e was further reduced to 6.4. In the presence of EIPA the entire graph is shifted to more acidic values. At pH_e 6.4 EIPA-treated cells were less rounded than the control cells. The number of lamellipodia per cell increased from 0.8 ± 0.3 cell^{-1} to 4.6 ± 0.5 cell^{-1} as pH_e decreased from pH 7.5 to pH 6.6 (Fig. 4*B*). It decreased to 2.0 ± 0.3 when pH_e was further reduced to 6.4. The application of EIPA caused a significant drop in the number of lamellipodia in cells that had been exposed to pH values varying between 6.6 and 7.5. Interestingly, in EIPA-treated cells the number of lamelliopodia continuously rose from 0 ± 0 to 2.5 ± 0.5 cell^{-1} as pH_e decreased from pH 7.5 to pH 6.4. At pH 6.4 the number of lamellipodia was the same in EIPA-treated and in control cells (2.5 ± 0.5 cell^{-1} and 2.0 ± 0.3 cell^{-1}, respectively). This finding suggests that the effect of NHE inhibition on the formation of lamellipodia can at least partially be compensated by lowering pH_e. Similar results were obtained when the morphology of MV3 cells was analysed under the same conditions 180 min after seeding (data not shown). Sodium propionate (15 mmol l^{-1}) had an even more distinct effect on the morphology than had an acid pH_e. SI dropped to 0.11 ± 0.01 and cells developed numerous long lamellipodia which they tended to shed (Fig. 3*C*). This effect could be reversed by the simultaneous application of HOE642 ($SI = 0.61 \pm 0.1$).

In the presence of rhodocetin cells developed none or only one lamellipodium and remained rather round (Figs 3*C* and 4). This suggests that the interaction between integrin $\alpha 2\beta 1$ and the extracellular matrix is needed to form processes.

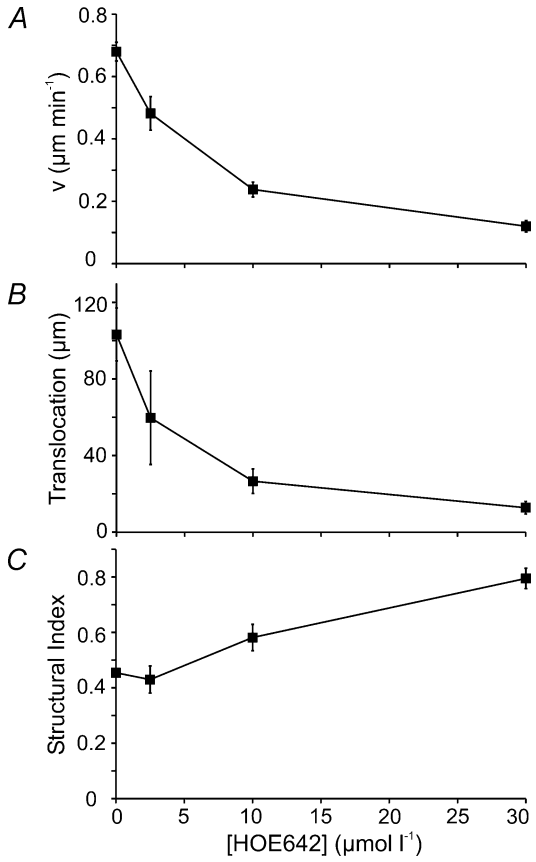

Figure 2. HOE642 affects the migratory speed (*v*), translocation and morphology (SI) of MV3 cells in a dose-dependent manner
pH_e was 7.0 throughout. $n = 20$–30 cells from three to five different trials in each case.

pH_e and NHE activity determine pH_i

The previous paragraphs showed that the extracellular pH and/or NHE activity have a strong impact on migration and morphology of MV3 cells. Thereupon we measured the resulting changes of the intracellular pH (pH_i) in order to determine whether they could account for the altered migratory behaviour. The results are summarized in Fig. 5. pH_i decreased as pH_e decreased. pH_i was 7.18 ± 0.01 ($n = 58$) in cells exposed to pH_e 7.5 while it was 6.58 ± 0.03 ($n = 59$) at pH_e 6.4. pH_i of HOE642 treated cells was 6.67 ± 0.01 ($n = 45$) at pH_e 7.2. pH_i of EIPA-treated cells was 6.78 ± 0.01 ($n = 21$) at pH_e 7.2 and it significantly decreased further to 6.71 ± 0.01 ($n = 29$) at pH_e 6.8. Thus, in contrast to migration, the effects of EIPA and extracellular acidification on pH_i are additive. After a 3 h exposure of MV3 cells to sodium propionate (15 mmol l^{-1}) at pH_e 7.0, pH_i was 7.1 ± 0.05 ($n = 38$ cells from four trials). Additional exposure of acidified cells to 10 μmol l^{-1} HOE642 led to a decrease in pH_i (pH 6.69 ± 0.04, $n =$ 30 cells from three trials).

It is conspicious that pH_i, migration and morphology of MV3 cells do not directly correlate with one another. An intracellular acidification caused by a low pH_e or by NHE inhibition is associated with completely different morphologies. Conversely, intracellular alkalinization by a high pH_e or intracellular acidification by NHE inhibition produce identical morphological changes. Similar discrepancies were found comparing control cells with propionate-treated cells. Thus, alterations of pH_i alone cannot explain the observed changes in migration and morphology.

Adhesion to the extracellular matrix increases as pH_e decreases

In this series of experiments we tested whether the observed changes in migration and morphology could be related to a pH_e- and/or NHE-mediated modulation of the cell–matrix interaction. To this end we performed adhesion assays at different pH_e values varying from 6.4

Table 1. The migratory behaviour of cells seeded on poly L-lysine does not depend on pH_e

	pH 6.6	pH 6.8	pH 7.2	pH 7.5
v (μm min^{-1})$_{coll}$	0.25 ± 0.02 (30)	0.45 ± 0.036 (30)	0.51 ± 0.036 (30)	0.24 ± 0.024 (30)
v (μm min^{-1})$_{poly}$	0.06 ± 0.007 (29)*	0.04 ± 0.005 (16)*	0.04 ± 0.005 (23)*	0.05 ± 0.004 (19)*
Translocation (μm)$_{coll}$	27.2 ± 5 (30)	61.3 ± 9.4 (30)	66.9 ± 10.1 (30)	20.7 ± 2.8 (30)
Translocation (μm)$_{poly}$	4.39 ± 0.41 (29)*	5.8 ± 0.8 (16)*	3.49 ± 0.69 (23)*	7.07 ± 0.54 (19)*
Structural index (SI)$_{coll}$	0.37 ± 0.02 (30)	0.34 ± 0.02 (30)	0.51 ± 0.02 (30)	0.73 ± 0.02 (30)
Structural index (SI)$_{poly}$	0.86 ± 0.02 (29)*	0.84 ± 0.03 (16)*	0.87 ± 0.03 (23)*	0.88 ± 0.01 (19)*

The number in parentheses represents the number of analysed cells from three different trials for poly L-lysine (poly) and up to five different trials for collagen (coll). *$P < 0.01$; poly L-lysine *versus* collagen.

to 7.5 in the presence and absence of EIPA (Fig. 6). The number of adhesive cells increased by 70% ($P < 0.02$) from 135 ± 20 cells/area ($n = 6$ trials) to 229 ± 27 cells/area ($n = 6$) as pH_e was lowered from pH 7.5 to pH 6.8. A further reduction of pH_e below pH 6.8, however, led to a slight decrease in the number of adhesive cells (194 ± 23 cells/area; $n = 6$). This decrease was not caused by acid-induced cell death or apoptosis since MV3 cells can easily be cultured at pH 6.6 for several months (data not shown). Inhibiting NHE with EIPA caused a significant drop in the number of adhesive cells by 44% at pH 6.4 up to 62% at pH 6.8. Interestingly, the adhesion of EIPA-treated cells continuously increased as pH_e decreased. This indicates that an acidic pH_e may compensate for the effect of NHE inhibition on cell adhesion. Cell adhesion could also be reduced by rhodocetin (Fig. 6). The number of adhesive cells upon rhodocetin treatment at pH_e 6.8 or 7.0 resembled that of untreated cells at pH_e 7.5.

The pH_e dependence of the cell–matrix interaction could as well be demonstrated in another set of experiments. Cells incorporated into a collagen matrix and exposed to low pH_e values (pH 6.8) pulled on the collagen matrix when they retracted their processes (Fig. 7). The cell-induced movement of the matrix was made visible by the displacement of microbeads that were incorporated in the matrix. Within 30 min the microbeads were displaced by 1.53 ± 0.27 μm at pH_e 6.8 ($n = 12$ beads from four different trials) as opposed to only 0.15 ± 0.05 when cells were observed at pH_e 7.5 ($n = 15$). These observations indicate that the cell surface/collagen interaction is stronger at lower pH_e values and weaker at higher pH_e values.

pH_e does not stimulate the expression of integrin β1

The integrin dimer $\alpha 2\beta 1$ mediates cell adhesion, spreading and migration in MV3 cells (Friedl *et al.* 1998; Maaser *et al.* 1999; Friedl & Bröcker, 2000). We therefore tested whether the pH_e-dependent strengthening of the cell–matrix interaction was due to a pH_e-dependent up-regulation of the integrin β1-expression. However, immunoblots revealed no pH_e induced differences in the overall expression of integrin β1 (Fig. 8). The intensity of the two integrin β1 bands at 110 and 130 kDa remained the same regardless of the pH_e cells had been exposed to prior to cell lysis.

Formation and distribution of focal adhesion sites are affected by pH_e

The distribution of vinculin, a cytosolic component of the focal contacts, was also affected by pH_e (Fig. 9*A*–*C*). Immunolocalization of the plasma membrane-associated vinculin revealed that it was more or less evenly distributed along the plasma membrane of cells exposed to pH_e 7.5. At pH_e 7.2 and 7.0 the vinculin was still rather evenly distributed but also appeared in a spotty fashion along the lamellipodia. At lower pH_e values it accumulated in a typically patchy pattern at the leading edges, i.e. the tips, of the lamellipodia. The distribution of integrin β1 did not fully correspond to that of vinculin. The integrin β1 in lamellipodia of cells exposed to lower pH_e at which stronger adhesion had been observed was hardly labelled (Fig. 9*F*). The incorporation of less integrin β1 into the plasma membrane appears to be an improbable cause for this phenomenon since the expression of integrin β1 does not depend on pH_e (Fig. 8) and since the traction forces exerted on the collagen fibres are higher at low pH_e (Fig. 7). We favour the explanation that the extracellular binding site for the function blocking antibody might be sterically blocked by collagen and therefore not accessible for the antibody.

Discussion

NHE activity plays a key role in cell migration. It is required for the migration of keratinocytes (Bereiter-Hahn & Voth, 1988), human leucocytes (Simchowitz & Cragoe, 1986; Ritter *et al.* 1998), neutrophil granulocytes (Rosengren *et al.* 1994), fibroblasts (Denker & Barber, 2002*b*) and renal epithelial (Madin-Darby canine kidney, MDCK-F) cells (Klein *et al.* 2000). NHE inhibition leads to a reduction in

the migration rate of MDCK-F cells (Klein *et al.* 2000) while NHE activation augments the motility and the invasiveness of human breast carcinoma cells (Reshkin *et al.* 2000). The present results are fully consistent with those findings showing a drastic impairment in cell motility of human melanoma cells in response to NHE inhibition by EIPA or HOE642.

Another key finding of the present study is that migration, morphology and adhesion or cell–matrix interactions mediated by integrin $\alpha 2\beta 1$ depend on pH_e. Modifying the pH_e changed pH_i as well. However, pH_e-induced modifications of pH_i can be ruled out as the only cause for the observed effects. Intracellular acidification was accompanied by either a round morphology and a low adhesion rate in the case of NHE inhibition or by a dendritic morphology and a higher adhesion rate upon exposure to a low pH_e. Conversely, cells were spherical regardless of whether pH_i was alkaline (in response to exposure to a high pH_e) or acidic (because of NHE inhibition). Moreover, cells were dendritic with an almost normal pH_i in the presence of sodium propionate, whereas they became spherical with an acidic pH_i after additional exposure to HOE642. The question arises what factors other than pH_e-induced modifications of pH_i

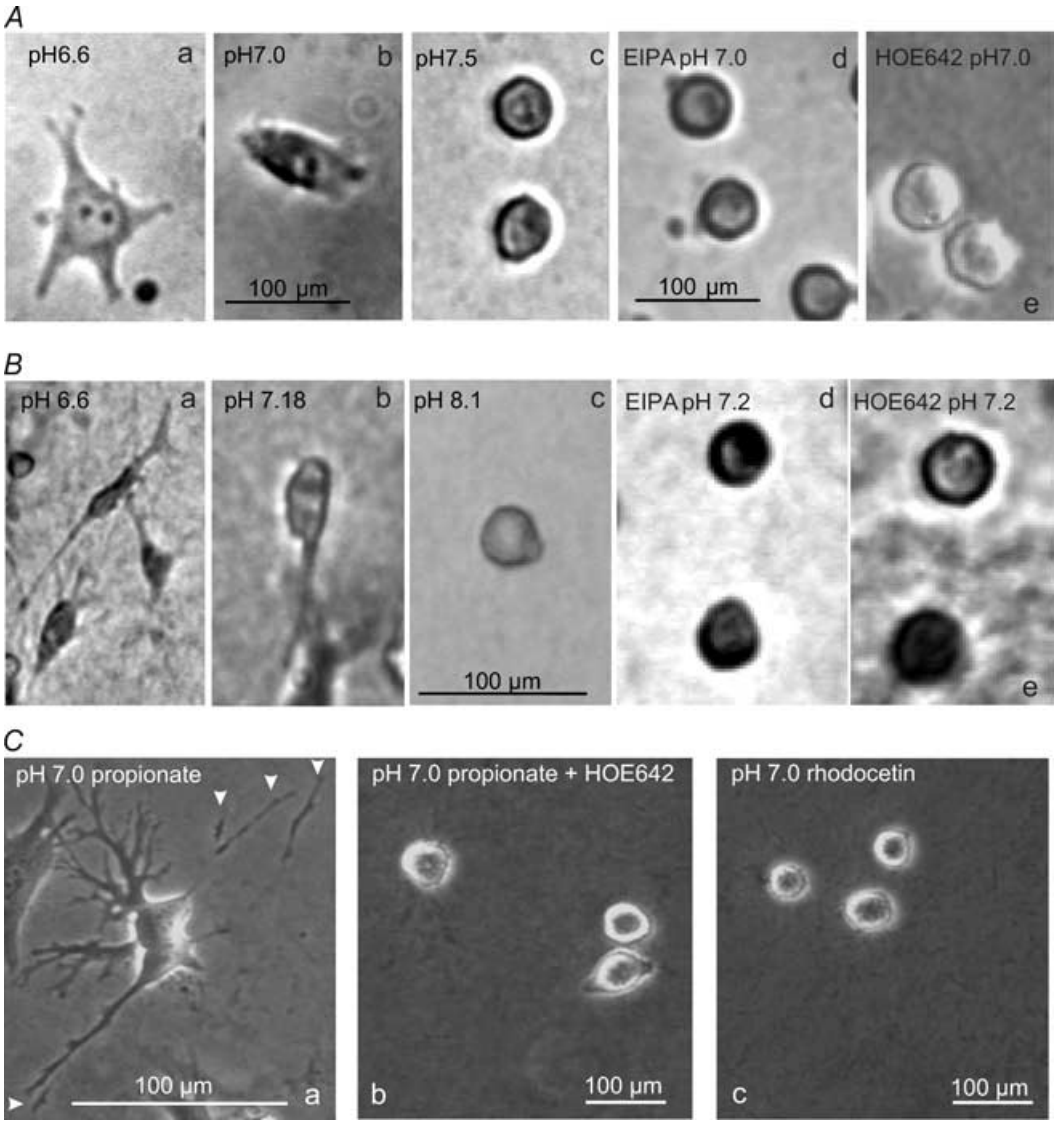

Figure 3. Morphology of MV3 cells
A and *B*, cells seeded on collagen matrices (*A*) or incorporated into collagen lattices (*B*) after a 3 h exposure to different pH_e values (*a*–*c*; Supplemental material videos 1–3) or 3 h after the application of 10 μmol l^{-1} EIPA (*d*; video 4) or 10 μmol l^{-1} HOE642 (e; video 5) at pH_e 7.2. *C*, cells seeded on collagen matrices were exposed to sodium propionate (*a*) or to sodium propionate plus HOE642 (*b*) or treated with rhodocetin (*c*). The arrow heads in *Ca* indicate shedding of cell processes.

may be involved. Needless to say, NHE activity is one candidate. NHE blockage or alkaline pH_e and pH_i result in low or no NHE activity, which causes the cells to round up. Acidic pH_e and pH_i or stimulation of the NHE by loading the cells with propionic acid result in high NHE activity leading to a dendritic cell shape and a high adhesiveness. Thus, it is obvious that there is a correlation between the NHE activity of human melanoma cells, their migration, morphology and adhesion. These observations are in line with previous studies showing that (i) a loss of the NHE1-dependent cytsokeletal anchoring impairs cell polarity and reduces the directionality in cell migration (Denker & Barber, 2002*b*), (ii) the transport activity of the NHE1 is stimulated during cell adhesion (Schwartz, 1992; Schwartz & Lechene, 1992), and (iii) NHE1 activity is necessary for the assembly of focal adhesions (Tominaga & Barber, 1998).

However, the present results provide evidence that pH_e itself contributes to the observed effects. The results point to a modulation of the cells' adhesiveness, i.e. to a modulation of the interaction between integrin $\alpha2\beta1$ and collagen I by pH_e. What is the experimental justification for this explanation? First, exposure of EIPA-treated cells to lower pH_e values leads to an increase in the cells' adhesiveness suggesting that the effects of NHE inhibition on cell adhesion can, at least partially, be neutralized by extracellular acidification (Fig. 6). Second, cells pull on the matrix at pH_e 6.8 as shown by the displacement of beads incorporated in the matrix whereas they do not displace adjacent beads at pH_e 7.5 indicating a rather tight cell surface–matrix interaction at lower pH_e values (Fig. 7). This experiment also demonstrates that extracellular acidification in the observed pH range does not reduce the contractility of MV3 cells. This is of interest since an acidic pH can exert effects on cell contractility by altering the structure, activity, or interaction of several actin-binding and cross-linking proteins such as the actin depolymerizing factor (Hawkins *et al.* 1993; Faff & Nolte, 2000), talin (Schmidt *et al.* 1993) or α-actinin (Condeelis & Vahey, 1982). Third, the number of lamellipodia in EIPA-treated cells increases as pH_e decreases (Fig. 4). It

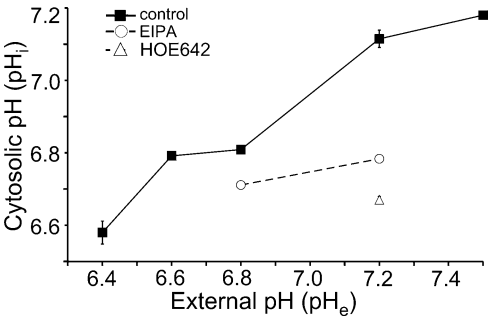

Figure 5. Cytosolic pH (pH_i) of MV3 cells depends on the external pH (pH_e) or NHE activity
pH_i was measured after a 3 h exposure to different pH_e values (■) or 3 h after the addition of 10 μmol l^{-1} EIPA (at pH_e 6.8 and 7.2; ○) and 10 μmol l^{-1} HOE642 (at pH_e 7.2; △). *n* varied between 21 and 106 cells from three to six trials.

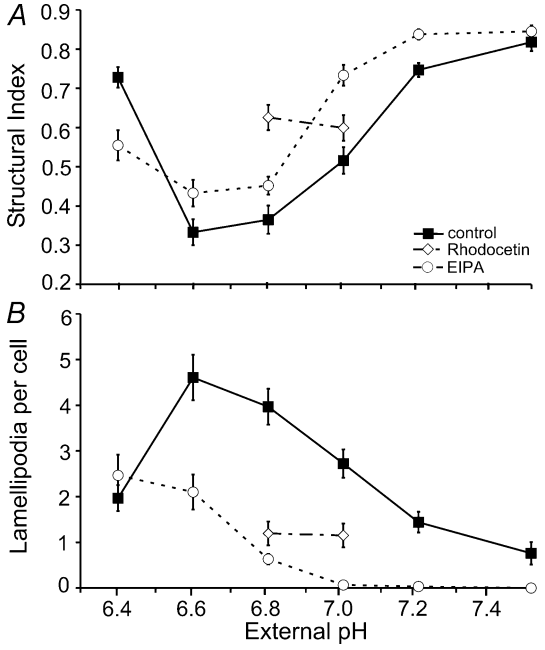

Figure 4. Structural index (*A*) and formation of lamellipodia (*B*) in MV3 cells depend on pH_e and NHE activity
Cells were seeded *on* collagen and incubated in RPMI$^-$ media of different pH_e in the presence (○) or absence (■) of 10 μmol l^{-1} EIPA or in the presence of 5 μg ml^{-1} rhodocetin (grey diamonds). The parameters were determined at $t = 60$ after seeding. The results shown in *A* and *B* were obtained from the same cells. Each data point represents the mean ± S.E.M. obtained from $n = 50$ cells from five different experiments (5 cells per area ($2 \times 10^5 \mu m^2$), 2 areas per experiment).

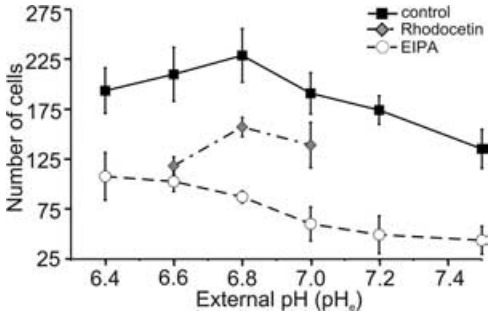

Figure 6. Adhesion of MV3 cells to a collagen matrix depends on pH_e and NHE activity
The adhesiveness is represented by the number of cells that remained stuck to the collagen matrix after washing with PBS 60 min after seeding. Cells were treated with rhodocetin (grey diamonds, $n =$ 3 trials, four areas per trial) or exposed to solutions of various pH_e with (○, $n = 4$ trials, two areas per trial) or without (■, $n = 6$ trials, two areas per trial) 10 μmol l^{-1} EIPA.

seems that at low pH_e values the lamellipodia cannot become detached from the matrix so that the affected cells remain stuck and hardly migrate while forming new processes that again can barely be retracted.

Fourth, although a rather soft finding, the present immunofluorescence stainings (Fig. 9) are in line with the previous arguments. Vinculin forming the cytoskeletal link between integrin β1-bound talin and other cytosolic components of focal adhesions such as tensin, paxillin and α-actinin (Zamir & Geiger, 2001) accumulates at the leading edges of lamellipodia at low pH_e while it seems to be evenly distributed along the membrane at pH_e 7.5. At the same time the access for the integrin β1 mAb to its extracellular epitope is impaired as pH_e decreases. This is consistent with the idea that a higher extracellular proton concentration increases the integrin/collagen binding force thereby sterically blocking the mAb's access to its binding site. Fifth, the expression of integrin β1 was not affected by pH_e (Fig. 8). Palecek *et al.* (1997) demonstrated that varying the quantitiy of integrins or its ligands has a strong impact on cell–substratum adhesiveness in CHO cells and thereby affects migration. We cannot completely rule out a pH_e-dependent incorporation of integrin β1 into the plasma membrane of MV3 cells. However, the pH_e-independent integrin β1-expression implies that besides the quantity of cell matrix interactions their binding strength, probably affected by pH_e, may also

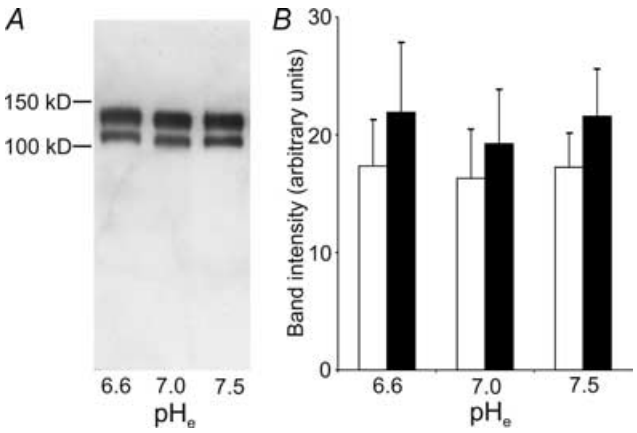

Figure 8. In MV3 cells the expression of integrin β1 does not depend on pH_e
A, Western blot of human integrin β1. Equal amounts of protein (2 μg) were loaded. *B*, the 110 kDa (precursor protein, open bars) as well as the 130 kDa bands (mature protein, filled bars) did not differ depending on pH_e (mean ± S.E.M.; $n = 5$ blots).

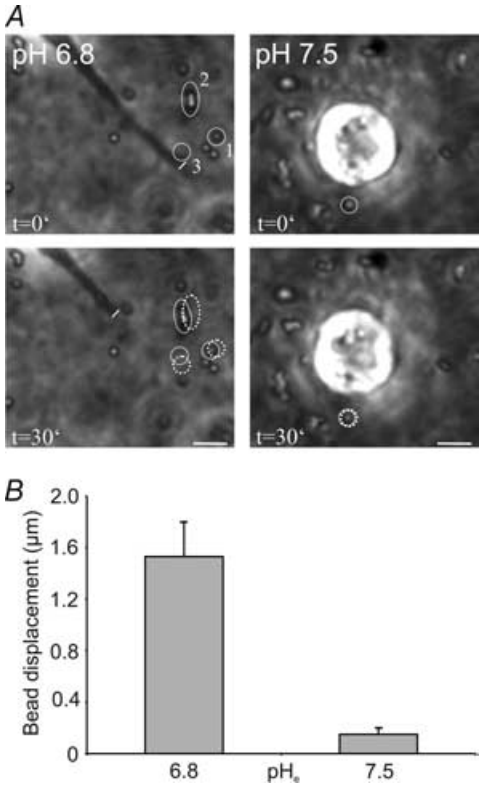

Figure 7. Cells exposed to low pH_e values (pH 6.8) pull on the matrix when they retract their lamellipodia
This is shown by the displacement of microbeads incorporated in the collagen matrix. *A*, bead *1* moved 1.1 μm within 30 min, beads *2* and *3* were displaced by 1.3 and 1.9 μm, respectively. At high pH_e (pH 7.5) cells did not exert traction on the matrix. The labelled bead moved 0.2 μm. Scale bar = 10 μm. *B*, statistics of bead displacement at pH_e 6.8 ($n = 12$ beads from four different trials, three beads per cell) and at pH_e 7.5 ($n = 15$ beads from five different trials, three beads per cell).

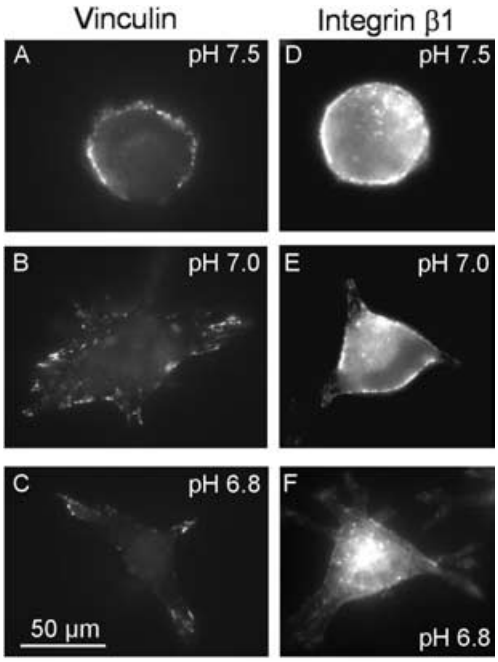

Figure 9. Comparison of the distributions of vinculin (*A–C*) and integrin β1 (*D–F*) in MV3 cells at different pH_e
Cells were seeded on collagen at different pH_e values and then fixed 60 min after seeding. pH_e varied between pH 6.8 and pH 7.5. Scale bar: 50 μm.

modify adhesion and migration. Sixth, applying atomic force microscopy Lehenkari & Horton (1999) found the pH optimum for the binding force of the fibronectin ligand-sequence GRGDSP to integrin $\alpha v\beta 3$ to be pH 6.5. This is consistent with the present finding that at pH_e 6.4 the binding loosens and the cells are of spherical shape. The NHE1 is very active at pH_e 6.4, which may decrease the local pH_e at the outer face of the plasma membrane to even lower values. When NHE is inhibited by EIPA at pH_e 6.4 no more protons are exported from the cytosol to the outer face of the plasma membrane and the local pH_e may be less acidic than it would be in the absence of EIPA. Consequently, cells are less spherical in the presence of EIPA.

Interestingly, the NHE and the integrin receptor molecules are often colocalized at the focal adhesion sites of the leading edges of lamellipodia (Grinstein *et al.* 1993; Plopper *et al.* 1995). Thus, the NHE could create a proton-enriched microenvironment in the immediate vicinity of the focal adhesion complexes, i.e. close to integrin molecules. In fact, protons can be laterally transferred along the surface of biological membranes. They move along lipid/water interfaces rather than diffusing away (Prats *et al.* 1986; Tessié *et al.* 1990). The current state of literature combined with the present observations led us to hypothesize that the local pH at focal adhesion sites may influence the strength of cell adhesion, i.e. of the integrin/collagen bond, and thereby affect cell migration (Fig. 10). A surplus of protons or a lively NHE activity would lead to a tight adhesion whereas alkalosis, a lack of protons or an inhibited NHE activity would prevent adhesion. Future experiments will have to verify this hypothesis and to show the existence of such a pH microenvironment at the outer surface of the plasma membrane.

Integrin binding to the extracellular matrix triggers a multitude of intracellular signals that are in part transmitted by the focal adhesion kinase (FAK) and the integrin linked kinase (ILK; Wu & Dedhar, 2001). They bind to integrin β tails (Liu *et al.* 2000). The phosphorylation state of FAK and its kinase activity are regulated by the binding of cells to the extracellular matrix (Schlaepfer & Hunter, 1998; Hauck *et al.* 2001; Hauck *et al.* 2002). On the assumption that extracellular protons stabilize the integrin–collagen bond, it is to be expected that at pH_e 7.5 (weak adhesion) no or less FAK is phosphorylated than at pH_e 6.6 (strong adhesion). Alternatively, other integrin pathways such as the RACK1–Src interaction (Cox *et al.* 2003) may be involved. Future studies will show if and how those signal transduction pathways starting from the integrin–collagen interaction are affected by the proton concentration at the cell surface. The binding of collagen to integrin $\alpha 2\beta 1$ is stimulated by Mg^{2+} and Mn^{2+} and inhibited by Ca^{2+} (Humphries, 2002). We are now trying to imitate the effects pH_e has on cell adhesion, migration and morphology by (i) varying the Mg^{2+}/Ca^{2+}

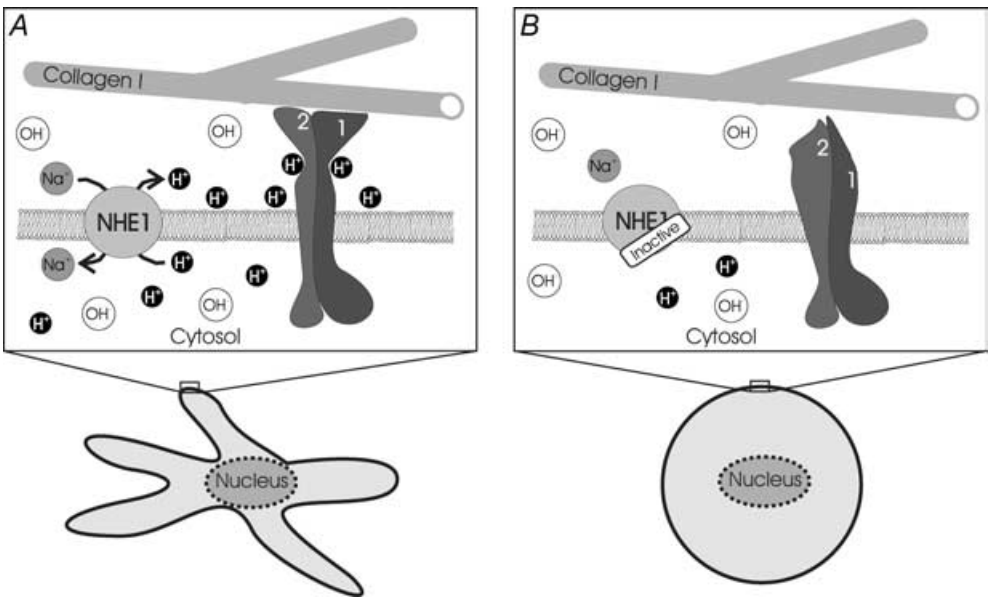

Figure 10. Hypothetical model of the integrin–collagen interaction
Integrins and NHE1 are colocalized. Protons stabilize the collagen–integrin ($\alpha 2\beta 1$ dimer) bond. *A*, acidosis, a surplus of protons or a lively NHE activity, leads to tight adhesion which generates a dendritic cell shape. *B*, alkalosis, a lack of protons or an inhibited NHE activity, prevents adhesion and cells become spherical.

ratio in the experimental solution and (ii) adding Mn^{2+}.

References

Beningo KA, Dembo M, Kaverina I, Small JV & Wang Y-L (2001). Nascent focal adhesions are responsible for the generation of strong propulsive forces in migrating fibroblasts. *J Cell Biol* **153**, 881–887.

Bereiter-Hahn J & Voth M (1988). Ionic control of locomotion and shape of epithelial cells. II. Role of monovalent cations. *Cell Motil Cytoskeleton* **10**, 528–536.

Boron WF (1983). Transport of H^+ and ionic weak acids and bases. *J Membr Biol* **72**, 1–16.

Brakebusch C & Fässler R (2003). The integrin-actin connection, an eternal love affair. *EMBO J* **22**, 2324–2333.

Condeelis J & Vahey M (1982). A calcium- and pH-regulated protein from *Dictyostelium discoideum* that cross-links actin filaments. *J Cell Biol* **94**, 466–471.

Cox EA, Bennin D, Doan AT, O'Toole T & Huttenlocher A (2003). RACK1 regulates integrin-mediated adhesion, protrusion, and chemotactic cell migration via its Src-binding site. *Mol Biol Cell* **14**, 658–669.

Denker SP & Barber DL (2002*a*). Ion transport proteins anchor and regulate the cytoskeleton. *Curr Opin Cell Biol* **14**, 214–220.

Denker SP & Barber DL (2002*b*). Cell migration requires both ion translocation and cytoskeletal anchoring by the Na-H exchanger NHE1. *J Cell Biol* **159**, 1087–1096.

Denker SP, Huang DC, Orlowski J, Furthmayr H & Barber DL (2000). Direct binding of the Na-H exchanger NHE1 to ERM proteins regulates the cortical cytoskeleton and cell shape independently of H^+-translocation. *Mol Cell* **6**, 1425–1436.

Dunn GA & Brown AF (1987). A unified approach to analyzing cell motility. *J Cell Scisupplement* **8**, 81–102.

Dunn GA & Brown AF (1990). Quantifying cellular shape using moment invariants. *Lecture Notes Biomathematics, Biol Motion* **89**, 10–34.

Eble JA & Tuckwell DS (2003). The $\alpha 2\beta 1$ integrin inhibitor rhodocetin binds to the A-domain of the integrin $\alpha 2$ subunit proximal to the collagen-binding site. *Biochem J* **376**, 77–85.

Egeblad M & Werb Z (2002). New functions for the matrix metalloproteinases in cancer progression. *Nature Rev* **2**, 161–174.

Faff L & Nolte C (2000). Extracellular acidification decreases the basal motility of cultured mouse microglia via the rearrangement of the actin cytoskeleton. *Brain Res* **853**, 22–31.

Freire E & Coelho-Sampaio T (2000). Self-assembly of laminin induced by acidic pH. *J Biol Chem* **275**, 817–822.

Friedl P & Bröcker E-B (2000). The biology of cell locomotion within three-dimensional extracellular matrix. *Cell Mol Life Sci* **57**, 41–64.

Friedl P & Wolf K (2003). Tumour cell invasion and migration: diversity and escape mechanisms. *Nature Rev* **3**, 362–374.

Friedl P, Zänker KS & Bröcker E-B (1998). Cell migration strategies in 3-D extracellular matrix: differences in morphology, cell matrix interactions, and integrin function. *Microsc Res Techn* **43**, 369–378.

Friedlander DR, Zagzag D, Shiff B, Cohen H, Allen JC, Kelly PJ & Grumet M (1996). Migration of brain tumor cells on extracellular matrix proteins in vitro correlates with tumor type and grade and involves alphaV and beta1 integrins. *Cancer Res* **56**, 1939–1947.

Griffiths JR (1991). Are cancer cells acidic? *Br J Cancer* **64**, 425–427.

Grinstein S, Woodside M, Waddell TK, Downey GP, Orlowski J, Pouyssegur J, Wong DCP & Foskett JK (1993). Focal localization of the NHE-1 isoform of the Na^+/H^+ antiport: assessment of effects on intracellular pH. *EMBO J* **12**, 5209–5218.

Gulledge CJ & Dewhirst MW (1996). Tumor oxygenation: a matter of supply and demand. *Anticancer Res* **16**, 741–749.

Hauck CR, Hsia DA, Ilic D & Schlaepfer DD (2002). v-SRC SH3-enhanced interaction with focal adhesion kinase at $\beta 1$ integrin-containing invadopodia promotes cell invasion. *J Biol Chem* **277**, 12487–12490.

Hauck CR, Sieg DJ, Hsia DA, Loftus JC, Gaarde WA, Monia BP & Schlaepfer DD (2001). Inhibition of focal adhesion kinase expression or activity disrupts epidermal growth factor-stimulated signaling promoting the migration of invasive human carcinoma cells. *Cancer Res* **61**, 7079–7090.

Hawkins M, Pope B, Maciver SK & Weeds AG (1993). Human actin depolymerizing factor mediates a pH-sensitive destruction of actin filaments. *Biochemistry* **32**, 9985–9993.

Helmlinger G, Sckell A, Dellian M, Forbes NS & Jain RK (2002). Acid production in glycolysis-impaired tumors provides new insights into tumor metabolism. *Clin Cancer Res* **8**, 1284–1291.

Humphries MJ (2002). Insights into integrin-ligand binding and activation from the first crystal structure. *Arthritis Res* **4**, S69–S78.

Jalali S, del Pozo MA, Chen K-D, Miao H, Li Y-S, Schwartz MA, Shy J-Y & Chien S (2001). Integrin-mediated mechanotransduction requires its dynamic interaction with specific extracellular matrix (ECM) ligands. *Proc Natl Acad Sci U S A* **98**, 1042–1046.

Klein M, Seeger P, Schuricht B, Alper SL & Schwab A (2000). Polarization of Na^+/H^+ and Cl^-/HCO_3^- exchangers in migrating renal epithelial cells. *J General Physiol* **115**, 599–607.

Lagarde AE, Franchis AJ, Paris S & Poyssegur JM (1988). Effect of mutations affecting $Na^+ : H^+$ antiport activity on tumorigenic potential of hamster lung fibroblasts. *J Cell Biochem* **36**, 249–260.

Lehenkari PP & Horton MA (1999). Single integrin molecule adhesion forces in intact cells measured by atomic force microscopy. *Biochem Biophys Res Commun* **259**, 645–650.

Liu S, Calderwood DA & Ginsberg MH (2000). Integrin cytoplasmic domain-binding proteins. *J Cell Sci* **113**, 3536–3571.

Maaser K, Wolf K, Klein CE, Niggemann B, Zänker KS, Bröcker E-B & Friedl P (1999). Functional hierarchy of simultaneously expressed adhesion receptors: integrin $\alpha 2\beta 1$ but not CD44 mediates MV3 melanoma cell migration and matrix reorganization within three-dimensional hyaluron-containing collagen matrices. *Mol Biol Cell* **10**, 3067–3079.

McLean LA, Roscoe J, Jørgensen NK, Gorin FA & Cala PM (2000). Malignant gliomas display altered pH regulation by NHE1 compared with nontransformed astrocytes. *Am J Physiol Cell Physiol* **278**, C676–C688.

Mitchison TJ & Cramer LP (1996). Actin-based cell motility and cell locomotion. *Cell* **84**, 371–379.

Palecek SP, Loftus JC, Ginsberg MH, Lauffenburger DA & Horwitz AF (1997). Integrin-ligand binding properties govern cell migration speed through cell substratum adhesiveness. *Nature* **385**, 537–540.

Plopper GE, McNamee HP, Dike LE, Bojanowski K & Ingber DE (1995). Convergence of integrin and growth factor receptor signaling pathways within the focal adhesion complex. *Mol Biol Cell* **6**, 1349–1365.

Prats M, Teissié J & Tocanne J-F (1986). Lateral proton conduction at lipid–water interfaces and its implications for the chemiosmotic-coupling hypothesis. *Nature* **322**, 756–758.

Reshkin SJ, Bellizzi A, Albarini V, Guerra L, Tommasino M, Paradiso A & Casavola V (2000). Phosphoinositide 3-kinase is involved in the tumor-specific activation of human breast cancer cell Na^+/H^+ exchange, motility, and invasion induced by serum deprivation. *J Biol Chem* **275**, 5361–5369.

Ritter M, Schratzberger P, Rossmann H, Wöll E, Seiler K, Seidler U, Reinisch U, Kahler CM, Zwierzina H, Lang HJ, Lang F & Wiedermann CJ (1998). Effect of inhibitors of Na^+/H^+ exchange and gastric H^+/K^+ ATPase on cell volume, intracellular pH and migration of human polymorphonuclear leucocytes. *Br J Pharmacol* **124**, 627–638.

Rosengren S, Henson PM & Worthen GS (1994). Migration-associated volume changes in neutrophils facilitate the migratory process in vitro. *Am J Physiol* **267**, C1623–C1632.

Rotin D, Steele-Norwood D, Grinstein S & Tannock IF (1989). Requirement of the Na^+/H^+ exchanger for tumor growth. *Cancer Res* **49**, 205–211.

Saadoun S, Papadopoulos MC, Hara-Chikuma M & Verkman AS (2005). Impairment of angiogenesis and cell migration by targeted aquaporin-1 gene disruption. *Nature* **434**, 786–792.

Schlaepfer DD & Hunter T (1998). Integrin signalling and tyrosine phosphorylation: just the FAKs? *Trends Cell Biol* **8**, 151–157.

Schmidt JM, Robson RM, Zhang J & Stromer MH (1993). The marked pH-dependence of the talin–actin interaction. *Biochim Biophys Res Commun* **197**, 660–666.

Scholz W, Albus U, Counillon L, Gogelein H, Lang HJ, Linz W, Weichert A & Scholkens BA (1995). Protective effects of HOE642, a selective sodium-hydrogen exchange subtype 1 inhibitor, on cardiac ischaemia and reperfusion. *Cardiovasc Res* **29**, 260–268.

Schwab A (2001). Function and spatial distribution of ion channels and transporters in cell migration. *Am J Physiol Renal Physiol* **280**, F739–F747.

Schwark JR, Jansen HW, Lang HJ, Krick W, Burckhardt G & Hropot M (1998). S3226, a novel inhibitor of Na^+/H^+ exchanger subtype 3 in various cell types. *Eur J Physiol* **436**, 797–800.

Schwartz MA (1992). Transmembrane signalling by integrins. *Trends Cell Biol* **2**, 304–308.

Schwartz MA & Lechene C (1992). Adhesion is required for protein kinase C-dependent activation of the Na^+/H^+ antiporter by platelet-derived growth factor. *Proc Natl Acad Sci U S A* **89**, 6138–6141.

Schwartz MA, Lechene C & Ingber DE (1991). Insoluble fibronectin activates the Na/H antiporter by clustering and immobilizing integrin $\alpha 5\beta 1$, independent of cell shape. *Proc Natl Acad Sci U S A* **88**, 7849–7853.

Simchowitz L & Cragoe EJ (1986). Regulation of human neutrophil chemotaxis by intracellular pH. *J Biol Chem* **261**, 6492–6500.

Tamariz E & Grinnell F (2002). Modulation of fibroblast morphology and adhesion during collagen matrix remodeling. *Mol Biol Cell* **13**, 3915–3929.

Tannock IF & Rotin D (1989). Acid pH in tumors and its potential for therapeutic exploitation. *Cancer Res* **49**, 4373–4384.

Tessié J, Prats M, LeMassu A, Stewart LC & Kates M (1990). Lateral proton conduction in monolayers of phospholipids from extreme halophiles. *Biochemistry* **29**, 59–65.

Tominaga T & Barber DL (1998). Na-H exchange acts downstream of RhoA to regulate integrin-induced cell adhesion and spreading. *Mol Biol Cell* **9**, 2287–2303.

Van Muijen GN, Jansen KF, Cornelissen IM, Smeets DF, Beck JL & Ruiter DJ (1991). Establishment and characterization of a human melanoma cell line (MV3) which is highly metastatic in nude mice. *Int J Cancer* **48**, 85–91.

Wahl ML, Pooler PM, Briand P, Leeper DB & Owen CS (2002). Intracellular pH regulation in a nonmalignant and a derived malignant human breast cell line. *J Cell Physiol* **183**, 373–380.

Webb DJ, Parsons JT & Horwitz AF (2002). Adhesion assembly, disassembly and turnover in migrating cells – over and over and over again. *Nat Cell Biol* **4**, E97–E100.

Williams BR, Gelman RA, Poppke DC & Piez KA (1978). Collagen fibril formation. *J Biol Chem* **253**, 6578–6585.

Wu C & Dedhar S (2001). Integrin-linked kinase (ILK) and its interactors: a new paradigm for the coupling of extracellular matrix to actin cytoskeleton and signaling complexes. *J Cell Biol* **155**, 505–510.

Yamagata M & Tannock IF (1996). The chronic administration of drugs that inhibit the regulation of intracellular pH: in vitro and anti-tumour effects. *Br J Cancer* **73**, 1328–1334.

Zamir E & Geiger B (2001). Molecular complexity and dynamics of cell-matrix adhesions. *J Cell Sci* **114**, 3583–3590.

Acknowledgements

We thank Dr Peter Friedl's laboratory (Rudolf-Virchow-Zentrum, Universität Würzburg) for teaching us how to create 3D collagen lattices and Dr Claudia Eder for fruitful discussions. J.A.E. receives a grant from the Wilhelm Sander-Stiftung (grant number: 2003.136.1). This work was supported by the Deutsche Forschungsgemeinschaft (grant number: 407/9/1).

Supplemental material

The online version of this paper can be accessed at:
DOI: 10.1113/jphysiol.2005.088344
http://jp.physoc.org/cgi/content/full/jphysiol.2005.088344/DC1
and contains supplemental material consisting of five videos: MV3 cells embedded in collagen at pH_e 7.35 (video 1), 6.75 (video 2), and 8.1 (video 3) or in the presence of either 10 μmol l^{-1} EIPA (video 4,) or 10 μmol l^{-1} HOE642 (video 5) at pH_e 7.18 in each case were recorded for 5 h. Frames collected every 10 min are displayed at a rate of 4 frames s^{-1}.

This material can also be found as part of the full-text HTML version available from http://www.blackwell-synergy.com